Single-Biomolecule Kinetics: The Art of Studying a Single Enzyme

Victor I. Claessen,[1] Hans Engelkamp,[2] Peter C.M. Christianen,[2] Jan C. Maan,[2] Roeland J.M. Nolte,[1] Kerstin Blank,[1] and Alan E. Rowan[1]

[1]Department of Molecular Materials and [2]High Field Magnet Laboratory, Institute for Molecules and Materials, Radboud University, Nijmegen 6525 ED, The Netherlands; email: k.blank@science.ru.nl, a.rowan@science.ru.nl

Annu. Rev. Anal. Chem. 2010. 3:319–40

First published online as a Review in Advance on March 11, 2010

The *Annual Review of Analytical Chemistry* is online at anchem.annualreviews.org

This article's doi: 10.1146/annurev.anchem.111808.073638

1936-1327/10/0719-0319$20.00

Key Words

single-molecule microscopy, enzyme kinetics, protein immobilization, bioencapsulation

Abstract

The potential of single-enzyme studies to unravel the complex energy landscape of these polymeric catalysts is the next critical step in enzymology. From its inception in Rotman's emulsion experiments in the 1960s, the field of single-molecule enzymology has now advanced into the time-resolved age. Technological advances have enabled individual enzymatic turnover reactions to be observed with a millisecond time resolution. A number of initial studies have revealed the underlying static and dynamic disorder in the catalytic rates originating from conformational fluctuations. Although these experiments are still in their infancy, they may be able to relate the topography of the energy landscape to the biological function and regulation of enzymes. This review summarizes some of the experimental techniques and data-analysis methods that have been used to study individual enzyme molecules in search of a deeper understanding of their kinetics.

1. INTRODUCTION

Since the formulation of Michaelis-Menten kinetics almost a century ago (1), investigators have felt that enzyme kinetics has been adequately described. And why not? If one doubles the amount of enzyme, the reaction speed also doubles. If more substrate is added, the rate increases until a saturation point is reached, at which the enzyme cannot turn over any faster. The basic Michaelis-Menten reaction scheme is discussed at length in every biochemical textbook, but we briefly recapitulate: A substrate molecule (S) combines with an enzyme (E) to yield an enzyme-substrate complex (ES), which then reacts to the enzyme-product complex (EP). Thereafter, the enzyme rapidly releases the product molecule (P) (Equation 1):

$$\mathrm{E} + \mathrm{S} \underset{k_{-1}}{\overset{k_1}{\rightleftharpoons}} \mathrm{ES} \overset{k_2}{\rightarrow} \mathrm{EP} \rightarrow \mathrm{E} + \mathrm{P}. \tag{1}$$

When mixing enzyme and substrate ([E] $\ll$ [S]), a steady state is attained after a very brief period, and the concentration of ES is proportional to the substrate concentration. The reaction velocity under these steady-state conditions can be described by the Michaelis-Menten equation (Equation 2):

$$v = \frac{v_{\max}[\mathrm{S}]}{K_M + [\mathrm{S}]}, \tag{2}$$

where $v_{\max} = k_2[\mathrm{E}]$ is the maximum reaction velocity of the enzyme and the Michaelis-Menten constant $K_M = \frac{k_{-1}+k_2}{k_1}$ quantifies the affinity of the enzyme for its substrate (provided that $k_2 \ll k_{-1}$, which is a common assumption).

The Michaelis-Menten equation holds for most enzymatic reactions, even when the reaction scheme is more complex and involves intermediates along the reaction pathway. Without diminishing the achievements of Leonor Michaelis and Maud Menten, however, it has been recognized that K_M and k_{cat} simply provide a phenomenological description of the enzymatic reaction and that a detailed understanding of the molecular process requires different approaches. To identify intermediates on the reaction pathway and to determine the corresponding rate constants, a number of methods—such as the measurement of pre-steady-state kinetics with stopped flow—have been developed. However, these measurements provide average rate constants for the whole ensemble of enzymes under study, providing only part of the picture.

By the early 1960s, Boris Rotman (2) had realized the potential of analyzing the catalytic reaction of individual enzyme molecules compartmentalized in the droplets of a water-in-oil emulsion. Individual enzyme molecules were statistically encapsulated together with a fluorogenic substrate in these emulsion droplets, and the amount of generated fluorescent product molecules was measured after several hours. Through the use of this innovative approach, the effect of a heat shock on the enzyme preparation was investigated, revealing that individual enzymes were either dead or alive, with no intermediate state. Rather than exhibiting different levels of activity, the individual enzyme molecules either retained full activity or were completely inactivated. This result could only have been obtained through examination of individual enzymes, and this method promised to answer important questions about the functioning of enzyme molecules that ensemble measurements could not resolve. Yet for the next 35 years this newborn field of research remained dormant. Boris Rotman was three decades ahead of his time. Only in the past two decades or so have there been sufficient improvements in sensitivity and time resolution to enable kinetic experiments on individual enzymes.

2. THE FLUCTUATING ENZYME MODEL

Generally, as molecules become more complex, they begin to exhibit (*a*) static disorder, the distribution of distinct properties among the general population of molecules, and (*b*) dynamic disorder, wherein the properties of an individual molecule fluctuate in time. In the case of enzymes, both static and dynamic disorder are directly related to the three-dimensional structure and the related dynamics of the amino acid polymer (3, 4). State-of-the-art single-enzyme kinetics experiments aim to shed light on the structure-function-dynamics relationships that relate to this disorder.

Aristotle might have agreed that a string of amino acids does not a functional protein make. The folding of the amino acid chain into a specific configuration is vital to the function of proteins. Even the so-called natively unfolded proteins fold into a defined structure upon binding to one of their ligands (5, 6). The requirement for a specific configuration is especially necessary for enzymes, which usually rely on a certain, very precise spatial coordination of specific amino acid residues to form an active site. Enzymes are a remarkable product of evolution because their specific configuration must be maintained in the presence of thermal motion, which constantly induces fluctuations in the amino acid chain (7). The experimental observation that each individual enzyme's activity is not constant in time (8–15) is easily explained by these fluctuations in the three-dimensional structure of the enzyme: The enzyme can appear in different conformations, each with its own specific activity. In addition to the observation that conformations may differ in terms of catalytic activity, it is now well established that conformational changes are essential in many enzymatic reactions. They can even be the rate-limiting step in the catalytic turnover cycle (16, 17).

The number of thermodynamically and kinetically accessible conformations, their relative probabilities, and their interconversion rates are defined by the energy landscape of the enzyme. As a result, the enzyme sometimes finds itself in a conformation in which it turns over many times before converting to a state with a lower activity (**Figure 1**), which explains the so-called memory effect that has been observed in single-molecule experiments (8, 12, 13, 18–20). The energy landscape, therefore, crucially determines the time series of events observed in single-enzyme experiments, and investigators are attempting to reconstruct the energy landscape for an enzyme from single-molecule time traces (21, 22).

The energy landscape of an enzyme, however, is not static; every modification in the enzyme, in its interaction with the substrate or in the environmental conditions, affects the energy landscape by lowering or raising barriers. As a consequence, regulation of enzymatic activity, for example,

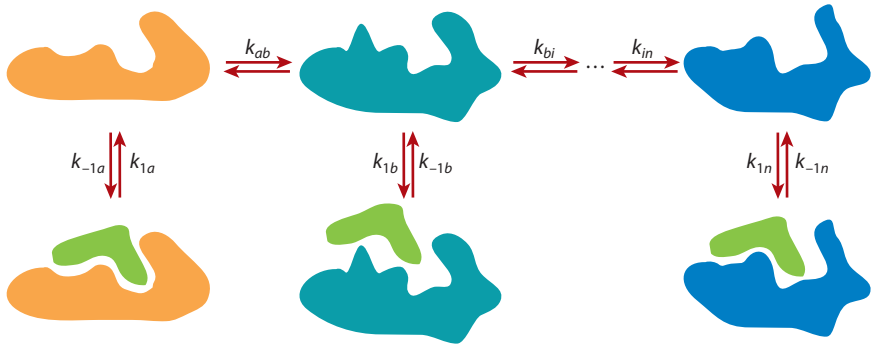

Figure 1

As an enzyme changes conformation, its affinity for a substrate changes, as does its ability to catalyze the reaction of substrate to product. As a result, the enzyme exhibits different rates in time.

may result from the (de)stabilization of a conformation with high activity (23). Evidence for this hypothesis has been obtained from nuclear magnetic resonance measurements and molecular dynamics simulations (4, 24). Several studies show that a ligand-bound conformation is sampled in the conformational ensemble with a certain probability, even if the ligand is not present. In these cases, ligand binding merely shifts the equilibrium toward the bound conformation (23, 25). Similar effects have been observed for the activation of proteins by phosphorylation (26, 27). Shifts in a conformational equilibrium may further originate from changes in the microenvironment, such as pH (28) and the presence of crowding agents (29). Moreover, mutations might stabilize or destabilize certain conformations, and evolution may proceed via the stabilization of an alternative enzyme conformation with altered activity or specificity (30).

In addition to all these biochemical modulators of enzyme function, physical influences are attracting increasing interest. For example, stretching forces may be an important regulator of biological activity for proteins with structural and mechanical function. Although studying the influence of forces on enzymatic reactions is technically challenging, several experimental single-molecule approaches have been developed. Initial studies show that an applied force indeed influences enzymatic activity (14, 31–33). On the basis of the limited data available to date, no general conclusions about the activating or deactivating effect of an applied force—which also greatly depends on the biological function of the enzyme under study—can yet be drawn.

The application of forces at the single-molecule level has recently been combined with single-molecule fluorescence detection (14, 31). This combination allows one to manipulate the enzyme landscape while simultaneously monitoring its activity, enabling one to study the effect of a force on an enzyme systematically. The next step in single-enzyme studies should focus on the systematic analysis of the influence of environmental, ligand binding, and mutation effects on the energy landscape and therefore on the enzymatic activity. This review focuses solely on the state of the art of fluorescence-based single-molecule approaches that directly monitor the catalytic reaction. Other versatile detection strategies based on single-molecule fluorescence resonance energy transfer that are designed to, for instance, monitor conformational changes, have been summarized in other recent reviews (34, 35). First, we describe applied detection technologies by means of prominent examples, together with the information obtained from these types of experiments. Second, we summarize the measurements performed with other enzyme-substrate systems, focusing on the main differences between these experiments, as well as the new information they have provided. Finally, we discuss future strategies that will allow us to study the above-mentioned regulation effects in, ideally, the enzymes' natural environment—the living cell.

3. TECHNIQUES

The activity of an enzyme is commonly monitored through the use of substrates that are converted to dye molecules during the enzymatic reaction. These dye molecules, which absorb light of a certain wavelength, accumulate over time, and the absorbance of the solution increases. The absorbance of an amassed pool of product molecules is readily observed, and such enzyme-activity measurements are the standard assay of classical enzyme kinetics. Adaptation of this approach to perceive the absorbance of a single product molecule is possible (36) but definitely impractical.

Enzyme substrates that are converted into fluorescent dye molecules provide a powerful alternative. Fluorescence detection works by illuminating the sample with a light source, usually either a lamp or a laser. This light is reflected by a long-pass dichroic mirror onto the sample, where it excites the fluorescent molecules. The fluorescent light emitted by these molecules passes through the same dichroic mirror and is detected either by a photomultiplier tube, a sensitive charge-coupled device (CCD) camera, or an avalanche photodiode (APD). Detection methods based

on fluorescence usually provide better signal-to-noise ratios and, as a consequence, much better sensitivity. Not only does state-of-the-art optical detector technology allow for the detection of picomolar concentrations of fluorescent dyes in a cuvette, it permits the identification of individual fluorescent dye molecules, a prerequisite for single-molecule experiments.

The identification of individual fluorescent dye molecules relies on the time-resolved detection of single photons emitted by the dye molecule. With modern detectors, tens of thousands of photons can be collected from a single fluorescent molecule every second, generating a large signal. However, this advantage for single-molecule fluorescence detection is also its biggest disadvantage because many types of molecules fluoresce or simply scatter light. Therefore, one must take care to eliminate contaminations. The number of different (contaminating) fluorophores that are detected can be limited by careful choice of the illumination source and the filter set, which restricts the excitation and emission wavelengths to the dye of interest. Also, the size and the geometry of the illuminated volume critically determine the number of contaminants that contribute to the detected signal. Several types of microscopy, which were invented to address this issue (**Figure 2**), are discussed in the following section. Once the contamination issue has been resolved, the only remaining requirement is to ensure sufficient spatial separation between the enzymes so that they can be inspected independently. In single-molecule studies, two is a crowd!

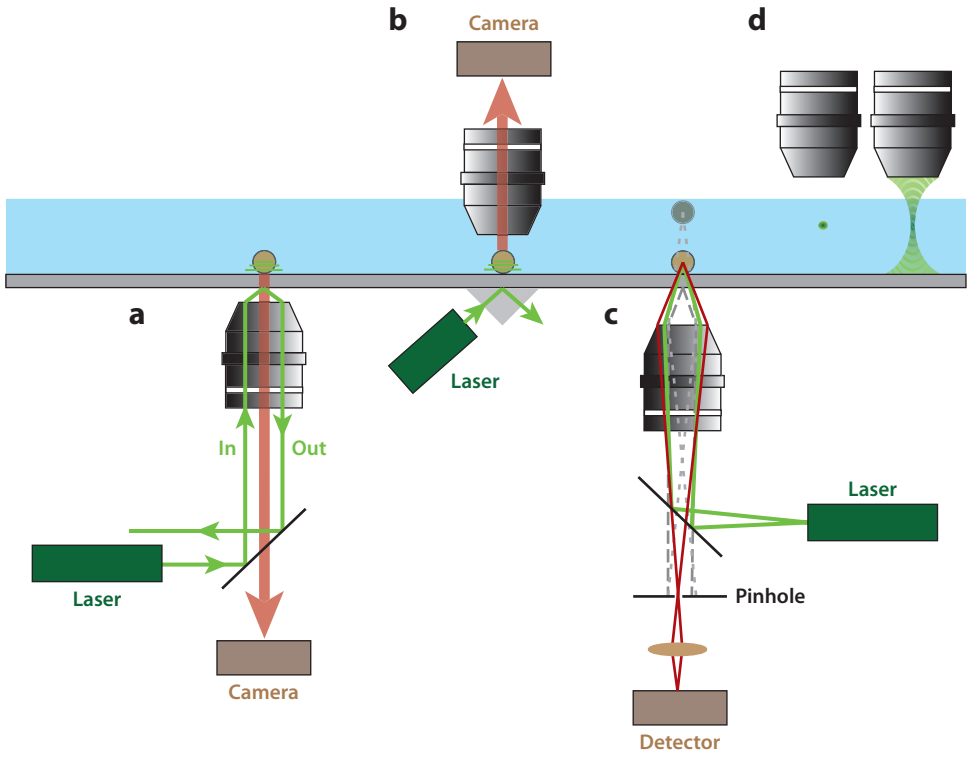

Figure 2

Principles of (*a*) objective-type total internal reflection fluorescence (TIRF), (*b*) prism-type TIRF, (*c*) confocal microscopy, and (*d*) a comparison of the illuminated areas in two-photon and single-photon excitation. In TIRF, only molecules close to the surface are illuminated and therefore detected. In confocal microscopy, a certain depth in the sample can be selected, and light from other layers is rejected by the pinhole.

3.1. Total Internal Reflection Fluorescence Microscopy

The total internal reflection fluorescence (TIRF) microscope was developed in the 1980s to overcome the problem of background fluorescence originating from molecules that were not bound to the surface of a sample glass slide. The principle is based on the fact that light is totally internally reflected from the glass-water interface when it strikes the interface under low angles. An evanescent wave of the light, however, penetrates into the water. This evanescent wave decays exponentially with the distance from the surface. As a result, only molecules very close to the surface (<100 nm) are excited. Therefore, the reduction of the penetration depth of the light into the sample allows the number of excited fluorophores to be minimized, resulting in a lower background signal.

TIRF microscopy was the first technique that showed single-fluorophore sensitivity applied to an enzymatic reaction (37). Enzymatically active, Cy5-labeled fragments of the molecular motor protein myosin were immobilized and localized on the surface, and the association-(hydrolysis-)dissociation reaction of individual Cy3-ATP(ADP) molecules was recorded with a camera. In contrast to freely diffusing Cy3-ATP, myosin-bound fluorescent molecules remained immobilized for a certain time. This keystone experiment represented a significant breakthrough for monitoring individual reaction events for the study of single enzymes. It has, however, one major drawback. Both substrate and product are equally fluorescent; thus, enzymatic turnovers cannot be fully quantified. That every binding event indeed corresponded to one catalytic reaction event was proven only indirectly by comparing the dissociation rate in the single-molecule experiment with the turnover rate for Cy3-ATP determined with ensemble measurements.

The power of this approach in the study of molecular motors has been demonstrated with a number of follow-up experiments. For example, by combining the TIRF microscope with optical tweezers, one can determine the time between the hydrolysis of one ATP molecule and the generation of force by the myosin molecule (31). This knowledge fills a gap in our understanding of the molecular mechanism of myosin. Similarly, Cy3-ATP-based experiments have also been applied to dissect details of the mechanism of the rotary motor F_1-ATPase (38, 39).

As in the above examples, TIRF excitation is coupled primarily with a CCD camera for detection. The advantage of this combination is that it allows a number of immobilized molecules to be monitored simultaneously. However, this benefit comes at the expense of a time resolution limited to the millisecond regime. Another disadvantage of TIRF, which is not shared by the techniques described below, is that a TIRF microscope can detect only molecules close to the surface.

3.2. Confocal Microscopy

A confocal microscope uses a laser that is focused into a diffraction-limited spot to reduce the size of the illuminated volume. Confocal microscopy shows a good signal-to-noise ratio and allows one to precisely adjust the focus in the z direction (40). Such adjustment can be achieved through the insertion of a pinhole into the emission light path in front of the detector. The pinhole blocks all the light originating from areas that are out of the microscope objective's focus. This strategy prevents out-of-focus light from reaching the detector and improves both the contrast and the resolution. The excitation light is also sent through a pinhole, ensuring that only the part of the sample that is in the detection focus is illuminated, which limits unnecessary bleaching in other parts of the sample.

Because the detection occurs in a single point, movement of the confocal volume over the sample is required to acquire an image. This can be achieved either by scanning the sample over a fixed beam (40) or by using mirrors to scan the beam across the sample. The latter approach

greatly improves the speed at which an image can be produced. By moving the microscope objective up and down, one can image several planes in the sample (from tens to several hundreds of micrometers deep) in succession to generate a three-dimensional image with a vertical resolution in the (low) micrometer range. Therefore, it takes longer to obtain information about the position of molecules on a surface, and the time to scan two subsequent images is slower than the frame rate of a CCD camera. When the catalytic activity of an individual enzyme molecule is being measured at a defined position, the time resolution of an APD detector—which is frequently used in confocal microscopes—is superior. Individual fluorescent dyes can be identified with submillisecond time resolution, which is better by at least a factor of ten than the best available CCD cameras.

The first application of confocal microscopy to individual enzymatic turnover reactions is described in a seminal paper by Xie and colleagues (8), who studied the enzyme cholesterol oxidase immobilized in an agarose gel. The active site of this enzyme contains a cofactor that is fluorescent in its oxidized form, but not in its reduced form. This cofactor is cycled between its oxidized and reduced forms in every reaction cycle, so every redox cycle was detected as an on/off cycle in the fluorescence measurement. Although this technique is certainly an elegant way of examining an enzyme—as it does not rely on artificial labeling, which might interfere with the enzyme's behavior—it is not widely applicable because most enzymes do not have a fluorescent cofactor.

The unique advantage of using the cofactor as the fluorescent reporter system is that one can determine not only the time of one complete turnover cycle, but also the durations of individual states along the turnover cycle (the oxidized, highly fluorescent state and the reduced, nonfluorescent state, respectively). To obtain the desired kinetic information, the authors (8) converted the fluorescence-intensity time trace into a binary on/off trajectory, which allowed for the determination of the durations of the oxidized (on) and reduced (off) states, respectively. The simplest method through which to perform such a conversion is to apply a threshold to the fluorescence time trace. Any level above the threshold is considered on; everything below it is considered off. The appropriate threshold level can be estimated from the photon-counting histogram. For traces with a high signal-to-noise ratio, as in the case of the cholesterol oxidase experiments, setting a threshold can be sufficient for separating the on and off levels. After the waiting times for the on and off levels have been determined, kinetic information is then obtained from the levels' respective probability distributions. The enzymatic turnover reaction may naïvely be considered as a stochastic process characterized by an exponential decay in the waiting-time distribution. In this case, one expects the data points to follow a linear pattern when plotting the histogram of the waiting times semilogarithmically. The waiting-time distribution in this experiment (8), however, deviated from this exponential behavior: More short waiting times were observed than would be expected from a purely stochastic process, meaning that the rate of reaction was apparently not constant in time.

More importantly, there was a correlation between successive on waiting times. This correlation manifested itself in the observation that short waiting times were more frequently followed by short waiting times and that long waiting times were more frequently followed by long waiting times. This so-called memory effect was depicted by a two-dimensional plot in which each waiting time was plotted against its preceding waiting time or the *n*th preceding waiting time (for an illustration, see Section 4.1.2). Similarly, the autocorrelation function of the waiting times (explained in more detail in the following section) shows a clear correlation over several waiting times. It is the observed memory effect that leads us to conclude that the enzyme remembers its previous conformational state and that the fluctuating enzyme model must be considered when describing this enzymatic reaction.

Autocorrelation analysis is applicable not only to the extracted waiting times. For cholesterol oxidase, it was also directly used on the intensity time trace. It provides an additional analysis method that does not require the use of a threshold. Similar to the waiting-time distribution, the intensity autocorrelation function could not be fitted to a single exponential, which would be expected for a first-order reaction. The intensity autocorrelation function thereby provides additional proof that more than one rate constant determines the catalytic reaction of cholesterol oxidase.

3.3. Fluorescence Correlation Spectroscopy

Autocorrelation analysis is normally used in fluorescence correlation spectroscopy (FCS), which was invented in the 1970s (41–44). Although FCS is not generally applicable to experiments on single enzymes, autocorrelation analysis is frequently used for single-enzyme time traces. In FCS, the molecules under study are not surface immobilized; rather, they diffuse freely through the confocal volume. The concentration of the sample is chosen such that there is only a small number (typically 1–100) of fluorescent molecules in the focus at one point in time. Every gain or loss of a fluorescent molecule in the focus causes the signal intensity at the detector to change. This experimental setup causes the measured fluorescence time trace to contain contributions from a large number of different molecules diffusing through the confocal volume. FCS, therefore, is not really a single-molecule technique, although the detection of individual molecules in the detection volume is certainly possible.

FCS allows one to measure the properties of molecules when the ensemble is in (dynamic) equilibrium (**Figure 3**). Fluctuations in fluorescence intensity can be directly related to changes in molecular properties originating from fluorescence blinking, intra- and intermolecular interactions, diffusion, and even enzymatic reactions. The autocorrelation function describes the fluctuations of the signal around the mean over a large range of time scales. It is defined as the average of the product of the variation around the mean and the variation around the mean some time τ later, divided by the mean squared:

$$g(\tau) = \frac{[\delta F(t)\delta F(t+\tau)]}{[F(t)]^2}. \quad (3)$$

Using this temporal correlation, one can obtain information about the time scale of the fluctuations by fitting the autocorrelation function with a suitable physical model that describes the origin of the observed intensity fluctuation. In studies of, for instance, the diffusion of molecules through a detection volume of known size, fitting the autocorrelation function gives the average diffusion speed (from which the hydrodynamic radius can be calculated) of the molecules and the concentration of these molecules in the solution. Autocorrelation can be calculated in real time by the multiple τ algorithm (45) or by simply binning the photons and correlating the binned fluorescence time trace. Furthermore, one can correlate the photon-arrival times directly, which allows the observation of correlations on a time scale faster than the bin size (46, 47).

Having worked in the area of FCS, Rigler and colleagues (9) performed a single-enzyme experiment with the enzyme horseradish peroxidase (HRP) and analyzed the results with autocorrelation analysis. Biotinylated HRP was immobilized on the surface of a streptavidin-coated cover slip. After adding the fluorogenic substrate dihydrorhodamine 6G, which is converted by the enzyme to yield the fluorescent dye Rhodamine 6G, the authors identified spots on the surface that had a higher fluorescence intensity than the rest of the surface. Also, the fluorescence signal fluctuated as a result of the enzymatic activity. Data measured at the position of these spots showed a different autocorrelation function than did data from the surface itself, where the autocorrelation

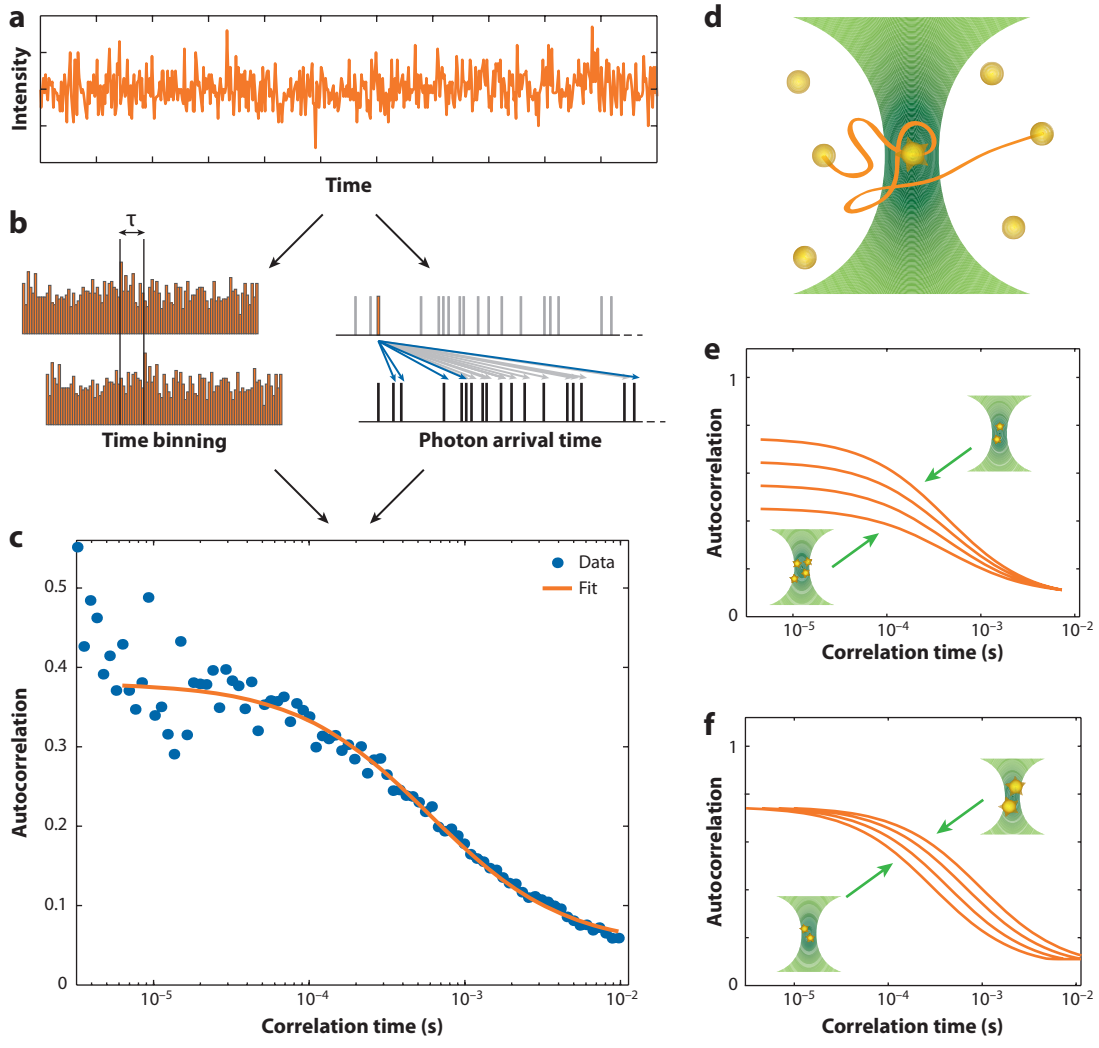

Figure 3

As molecules move in and out of the focus (*d*) of a microscope objective, the recorded fluorescence intensity signal (*a*) fluctuates. By autocorrelating this fluorescence intensity—either via correlation of the binned signal (*b*, *left*) or via direct correlation of the photon arrival times (*b*, *right*)—one can obtain the autocorrelation function (*c*). Two parameters can be obtained from the fit: the correlation time, which is related to the diffusion constant, and the correlation coefficient, which is related to the concentration. An increase in concentration leads to a decrease in the correlation coefficient (*e*) because the passing of an individual molecule contributes less to the total intensity and the fluctuation is therefore smaller. An increase in molecule size gives rise to longer correlation times (*f*) because each molecule resides for a longer time in the confocal volume.

function was flat. Time traces of more than 100 enzyme molecules were recorded and analyzed by autocorrelation. Within the duration of the experiment, the individual enzyme molecules showed a large distribution of rates for the formation of the enzyme-product complex (static disorder). Furthermore, as in the experiment with cholesterol oxidase, the autocorrelation functions could not be fitted with a single exponential; rather, a stretched exponential was introduced to obtain a good fit. A stretched exponential is characteristic of dynamic disorder, meaning that a large

number of different rate constants contribute to the reaction of a single enzyme. This HRP experiment provides additional proof that autocorrelation analysis is a powerful way to characterize the behavior of individual enzyme molecules and that a similar fluctuating enzyme model probably also describes the catalytic reaction of HRP. This conclusion is further supported by a subsequent, more detailed analysis of the data (18).

4. STRATEGIES FOR SINGLE-ENZYME EXPERIMENTS

Following the breakthrough experiments described above, several other enzymes were analyzed through the detection of either the turnover of a fluorogenic substrate or the redox state of a cofactor. Despite the many approaches used, all these systems exhibit static and/or dynamic disorder upon analysis, and each of the experiments has expanded our knowledge of single-enzyme behavior. An issue that has been addressed in all these follow-up experiments is that of immobilizing and identifying the enzymes on a surface. Every immobilization and labeling procedure may introduce disorder into the system due to interactions with the surface or the label.

4.1. Surface Immobilization

In the following sections, we discuss the different immobilization methods and describe the main differences between the experiments. We also describe attempts to avoid direct contact of the enzyme with a surface, such as the encapsulation of individual enzyme molecules in micro- or nanosized containers.

4.1.1. Nonspecific adsorption of the enzyme. Velonia et al. (11) deposited single molecules of *Candida antarctica* lipase B (CalB) on a glass surface that was made hydrophobic by functionalization with dichlorodimethylsilane. The enzyme molecules bound to the surface because of hydrophobic interaction. To achieve localization of the enzymes, the authors labeled the enzyme with a fluorescent dye; CalB does not turn over substrate molecules fast enough to allow for its localization from the accumulation of fluorescent product molecules in its proximity. After localizing an individual enzyme and placing it into the confocal volume, Velonia et al. used the confocal laser to bleach the fluorescent label, and individual turnovers were subsequently detected. A significant fraction of the enzymes, however, were found to be inactive, possibly because the molecules were partly denatured, a result of the interaction with the hydrophobic surface. Alternatively, some of the lipase molecules, which naturally bind to hydrophobic surfaces, may have been oriented with the active site toward the surface, thereby preventing any substrate molecules from entering and reacting.

Despite the problems encountered in this experiment, the active CalB molecules were measured for a much longer time than was possible in previous experiments (>20 min). As a result, by adding fresh substrate solution with increasing concentration, the authors were able to study the same single enzyme at several substrate concentrations. Above a concentration of ~1 μM 2′,7′-bis-(2-carboxy-ethyl)-5-(and -6-)carboxyfluorescein, acetomethyl ester (BCECF, AM) the addition of substrate did not result in significantly higher enzyme activity. A Michaelis-Menten plot for an individual enzyme molecule showed typical saturation behavior as predicted by Michaelis-Menten kinetics, suggesting that the Michaelis-Menten equation is valid at the single-molecule level. The determination of the Michaelis-Menten plot was complicated by the solubility limit of BCECF, AM, which is relatively hydrophobic. The long time traces, however, did not only allow the authors (12) to vary the substrate concentration, they also provided a high number of turnovers for the subsequent analysis of the waiting times between individual turnovers. CalB activity shows the

typical fingerprint of dynamic disorder as well as a very pronounced memory effect: CalB activity is clearly separated in phases with very high activity and in phases where almost no enzymatic turnovers occur at all. Surprisingly, the enzyme was predominantly inactive; the active phases constituted only 3% of the overall measurement time (11, 14).

4.1.2. Site-directed enzyme adsorption via a "protein foot." To overcome the previously encountered problems caused by nonspecific adsorption of CalB to the hydrophobic surface, a strategy to allow site-directed adsorption of the lipase from *Thermomyces lanuginosa* (TLL) was developed (19). The lipase was "clicked" (i.e., coupled via 2+3-Huisgen cycloaddition) to bovine serum albumin (BSA). A defined position was chosen for this coupling reaction in both proteins, resulting in well-defined heterodimers. BSA is known to adsorb to hydrophobic surfaces, whereas TLL is less hydrophobic than CalB. The TLL-BSA heterodimer, therefore, prefers to orient itself with the BSA toward the hydrophobic glass when adsorbing to the surface. This strategy protected the enzyme from surface-induced denaturation and ensured that the enzyme was oriented with its active site toward the solution. The BSA also presented an anchor for the attachment of a fluorescent label without any further modification of the enzyme itself. The authors localized the labeled enzyme-BSA heterodimers by scanning the surface with the confocal microscope and then adding a 1-μM solution of the fluorogenic substrate 5(6)-carboxyfluorescein diacetate. Nearly all the enzymes, which were identified with the help of the fluorescent label, were active, and the average turnover was 17 s^{-1}.

Again, the analysis of the waiting times between turnovers revealed that the distribution of waiting times was not completely random (**Figure 4**). Short waiting times were more often followed by short waiting times, and long waiting times were most often followed by long waiting times. For TLL, this memory effect lasts for more than 15 turnovers, which is an extremely long time. This strong correlation provides a clear indication for the fluctuating enzyme model. As long as the enzyme is in the same conformation, it produces product molecules with a characteristic rate. Once it switches to another conformation, the rate changes. This TLL study was the first experiment in which the enzyme was immobilized to the surface in a site-specific way. It is therefore unlikely that any additional heterogeneities were introduced into the system by the experimental design. Fluctuations in the rate constants must be an intrinsic property of the enzyme itself.

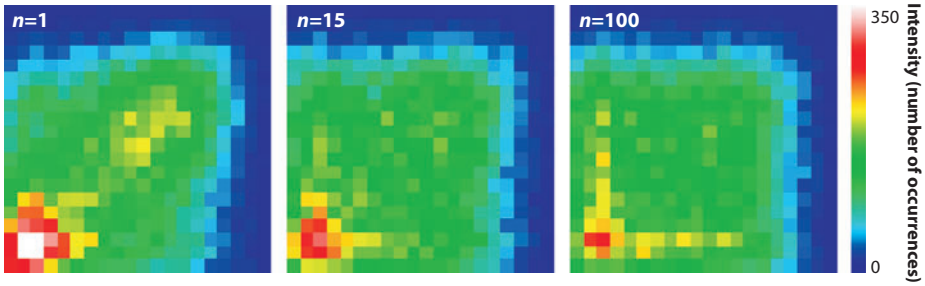

Figure 4

Two-dimensional correlation histograms of events separated by n events. Scales on the x and y axes range from 2 to 300 ms (logarithmic); the intensity range spans from 0 (*blue*) to 350 (*red*) occurrences (linear). The diagonal feature, which is clear in $n = 1$ and still present at $n = 15$ but not at $n = 100$, indicates the correlation between events. Because of the memory effect, short waiting times are more often followed by short waiting times, and long waiting times are more often followed by long waiting times. Reprinted with permission from Reference 19.

4.1.3. Site-specific and covalent enzyme immobilization. Site-specific immobilization was also used for the single-molecule analysis of the enzyme nitrite reductase (NiR) from *Alcaligenes faecalis* (48). NiR is a trimer with two copper centers per monomer, each involved in the catalytic reaction. An electron is accepted from a donor molecule by the type 1 copper center, transferred to the type 2 copper center, and subsequently used to reduce nitrite (NO_2^-) to nitric oxide (NO). In contrast to cholesterol oxidase, the copper cofactors are not fluorescent; neither are the substrate or product molecules. A different detection strategy was therefore necessary. This detection strategy was based on the broad absorption spectrum of the type 1 copper center when it is in its oxidized state. The oxidized type 1 copper center acted as a quencher for a fluorescent dye (ATTO655) that was coupled to the enzyme site-specifically in Förster distance to the copper center. As a result, the ATTO655 dye was fluorescent in the reduced state of the copper ion. Measuring the change in fluorescence emission of ATTO655 allowed the oxidation and reduction of the copper center to be followed.

To achieve immobilization to the surface, a mutant of NiR containing a surface-accessible cysteine was prepared. This mutant was coupled to a mercapto-functionalized glass surface via a short homobifunctional polyethylene glycol spacer with thiol-reactive end groups. In this experiment (48), the ATTO655 label was used to identify enzymes on the surface. Autocorrelation analysis of the recorded single-molecule traces yielded $K_M = 31 \pm 17$ μM and $k_{cat} = 6.5 \pm 2\ s^{-1}$. These values correspond well to the values measured at the ensemble level ($K_M = 50 \pm 20$ μM and $k_{cat} = 8 \pm 1\ s^{-1}$). This agreement proves that in this system the surface immobilization did not result in an altered enzymatic activity. As in the above-described experiments, the turnover rate of a single NiR enzyme varied over an order of magnitude, as indicated by the stretch parameter of the correlation fit. This result was intriguing because this enzyme is known from X-ray spectroscopy to have nearly superimposable conformations for the reduced and oxidized states as well as for the substrate- and product-bound states. The authors attributed the rate distribution to local variations in the coordination spheres of the copper centers. If they exist at all, the conformational fluctuations may be restricted to the close surroundings of the copper centers rather than to greater structural variations in the protein at large.

4.1.4. Enzyme immobilization via receptor-ligand interactions. Agreement of the kinetic constants K_M and k_{cat} between single-molecule and ensemble experiments has also been found for the enzyme β-galactosidase (13). Similar to the HRP experiment by Rigler et al. (9), biotinylated β-galactosidase was used for the immobilization. In contrast to HRP, β-galactosidase was not immobilized to the surface directly but rather to a streptavidin-containing bead, which was subsequently deposited on a biotin-containing surface. The attachment to the bead provided another interesting strategy with which to localize enzyme molecules because the bead can easily be observed with difference interference contrast microscopy. Subsequent placement of the confocal volume at the position of the bead allowed the turnover of the fluorogenic substrate resorufin-β-D-galactopyranoside (RGP) to be recorded. RGP has a relatively high solubility in an aqueous buffer; therefore, much higher substrate concentrations (up to 380 μM) could be used. Use of these high-substrate concentrations required the autohydrolysis of the substrate to be considered. Product molecules originating from autohydrolysis diffuse through the confocal volume and are detected as product molecules generated by the enzyme. To account for this problem, a second strong, defocused laser beam was used to illuminate a 100-μm-diameter area around the bead to bleach any resorufin molecules in its proximity.

After the data at different substrate concentrations were obtained, the corresponding waiting-time distributions of the off-times were analyzed. At very low substrate concentrations, the off-times were fitted by a single exponential function, whereas they became increasingly

multiexponential at higher substrate concentrations. This discrepancy can be explained with the fact that at low substrate concentrations the diffusion of the substrate to the enzyme is rate-limiting. Unfortunately, the substrate concentration could not be increased to K_M or higher because the enzymatic reaction proceeded so fast that individual turnovers could no longer be resolved. Despite the high solubility of RGP, the highest substrate concentration (100 μM) that could be used was approximately one-fourth of K_M (380 μM). On the basis of the available data points, an agreement of K_M and k_{cat} for single-molecule and ensemble measurements was obtained, and the validity of the Michaelis-Menten equation at the single-molecule level was affirmed. However, the shape of the waiting-time distribution at saturating substrate concentrations remains undiscovered and is difficult to determine with the currently available fluorogenic substrates because of solubility or autohydrolysis problems.

4.1.5. Immobilization of the substrate. It is not necessary to limit an experiment to immobilization of the enzyme; in some experiments, it is also possible—perhaps preferable—to immobilize the substrate. Especially for insoluble substrates such as lipid and phospholipid layers, as well as for high-molecular-weight substrates such as DNA, immobilization of the substrate provides an important means of observing the catalytic reaction. For instance, the use of wide-field microscopy allows one to simultaneously observe and track a number of individual phospholipase molecules while they eat their way through a phospholipid bilayer (49). In this study, both the enzymes and the phospholipid layer were fluorescently labeled so that the disappearance of the layer could be related to the presence of an enzyme. Although the experiment did not yield the precise rate of the catalytic reaction, it showed that the enzymes preferred the edge of the phospholipid layer, revealing that these layers are cleaved starting from defects.

More direct information about the rate of the catalytic reaction was obtained for the cleavage of DNA by the enzyme λ-exonuclease, which cleaves one strand of double-stranded DNA (dsDNA) successively from its 5′ end, yielding single-stranded DNA (ssDNA). When DNA was stretched on the surface under flow conditions, ssDNA appeared shorter because it coiled up. Because an increasing fraction of the dsDNA was converted to ssDNA, the DNA shortened; this shortening was detected by the movement of a bead attached to the DNA (10). This detection principle only works with long DNA polymers—16 μm in this case—that are long enough to extend (well) beyond the diffraction limit of optical microscopy. Analysis of the bead movement allowed the authors to allocate the melting of the 5′ base as the rate-limiting step of the reaction and furthermore again revealed dynamic disorder in the system. This experiment can be easily extended to fluorescence detection by labeling the DNA strand. This approach was recently used in a detailed analysis of DNA replication (50).

4.2. Gel Entrapment of Enzymes

The entrapment of enzymes in gels is a fast and easy way to immobilize enzymes. Gels possess interesting qualities, such as their ability to retain molecules without binding them chemically. They have a porous network for easy diffusion of substrates, and depending on the type of gel, the properties of the pores can be fine-tuned if necessary. Entrapment in agarose gels has frequently been used for biomolecules studied at the single-molecule level, for example in the Xie group's (8) experiment with cholesterol oxidase. Following gelation of an enzyme-containing agarose solution, a polarization measurement showed that the enzyme molecules were freely rotating while immobilized in the gel. This measurement demonstrates that the enzymes are not bound to the polymer matrix and that the smaller substrate molecules can most likely freely diffuse through the gel to reach the enzyme molecules.

More recently, an agarose gel was used to immobilize the enzyme chymotrypsin for single-molecule experiments with the fluorogenic substrate (suc-AlaAlaProPhe)$_2$–Rhodamine 110 (51). In addition to the typical fluctuations related to dynamic disorder another effect was observed: Enzymatic activity switched off several times for a relatively long time before the activity disappeared completely. This behavior was attributed to a multistep deactivation mechanism that was more complex than a simple transition from a fully active enzyme molecule to an inactive one.

Aside from agarose gels, sol-gels may be particularly well suited for the immobilization of enzymes. Owing to their excellent optical properties and controllable pore size, sol-gels have been extensively used for the entrapment of enzymes (e.g., lipases) for organic chemistry applications (52). Interestingly, for sol-gels, changes in enzyme properties (e.g., increases in activity or stability) have been observed, indicating that an interaction between the enzyme and the sol-gel takes place. This interaction may be an unwanted effect. The analysis of sol-gel-encapsulated enzymes at the single-molecule level may, however, be a way to study environmental influences on enzymatic activity.

4.3. Encapsulation in Containers

Individual enzyme molecules can also be encapsulated in micro- or nanosized containers such as vesicles, micelles, emulsion droplets, polymersomes, and virus capsids. These containers can then be fixed in space while the enzyme freely diffuses inside the container. This method of encapsulation may closely resemble biologically relevant conditions in which enzymes are frequently confined in small concentrations in subcellular compartments. Alternatively, small and sealable wells can be fabricated with micro- and nanofabrication techniques.

4.3.1. Encapsulation in a virus capsid. In an exotic but successful encapsulation strategy, individual HRP molecules were incorporated into virus capsids (53). After removal of its RNA, cowpea chloritic mottle virus (CCMV) particles turn into biocompatible containers with an outer diameter of 28 nm and an inner-cavity diameter of 18 nm. The shell consists of 180 protein subunits, which can be reversibly disassembled and reassembled by changing the pH and ionic strength of the buffer. Following reassembly of the capsid in the presence of a low concentration of enzyme molecules, a distribution of empty capsids and capsids filled with a single enzyme was obtained, just as in the trendsetting emulsion experiment performed by Rotman (2). The virus capsids were deposited onto a glass surface, where the capsid protected the enzyme from touching the surface. Enzymatic activity inside the virus capsid was detected with a confocal microscope through the use of dihydrorhodamine 6G as a fluorogenic substrate (**Figure 5**). The product accumulated in the inner cavity of the capsid, and a direct analysis of single turnovers was impossible. Autocorrelation analysis showed that diffusion of the product out of the capsid was almost 1000 times slower than unhampered diffusion. The rate of diffusion was increased two- to threefold by raising the pH, which swells the capsid and enlarges its pores.

Interestingly, in a control experiment in which fully assembled but empty capsids were mixed with HRP, some enzyme molecules nonspecifically absorbed to the outside of a capsid; that is, the capsid functioned as a so-called protein foot. The fluorescence intensity traces recorded from those molecules showed single events because there was no possibility of product accumulation.

4.3.2. Encapsulation in emulsion droplets. The virus experiment reveals one of the main characteristics of encapsulation in small containers. Unlike encapsulation in gels, in which substrate and product molecules can diffuse more or less freely, molecules may become (partially) entrapped inside the container together with the enzyme. This is not necessarily a problem: If the container is permeable neither for the substrate nor for the product, product molecules accumulate as the

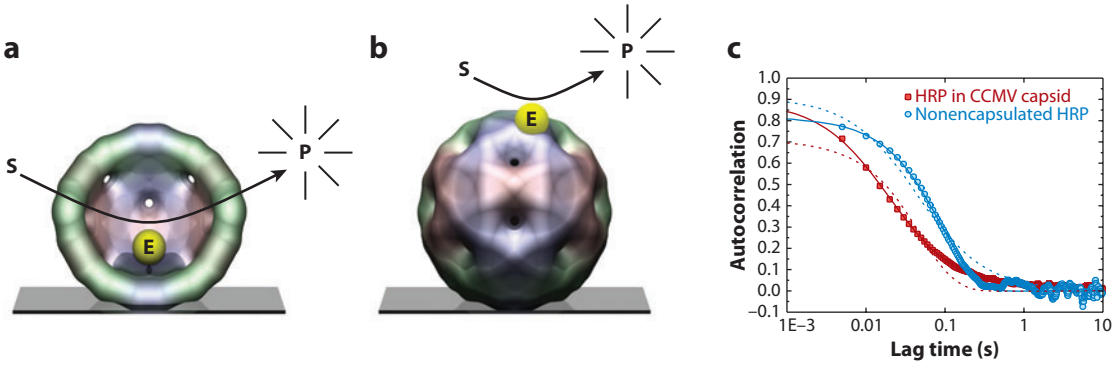

Figure 5

Illustration of the enzyme (E; *a*) encapsulated in the capsid and (*b*) adsorbed on the outside of the capsid. (*c*) Autocorrelation analysis reveals that the encapsulated enzyme (*red*) is diffusion limited in its substrate supply, as judged from the fit of a diffusion model (*solid line*) versus a single exponential fit (*dotted line*). In contrast, the enzyme on the outside (*blue*) fits to the single exponential (*solid line*), but not to the diffusion model (*dotted line*), indicating normal reaction kinetics. Abbreviations: CCMV, cowpea chloritic mottle virus; HRP, horseradish peroxidase; P, product molecule; S, substrate molecule. Reproduced from Reference 53.

enzymatic reaction proceeds, and the increasing product concentration can be determined as a function of time. This can be achieved for the droplets of a water-in-oil emulsion, for example, whose properties can be tuned such that all molecules in the water droplet are retained inside the droplet. This is the approach, followed by Rotman (2), that was briefly mentioned in the introduction. Rotman developed a method to study emulsified droplets made from an aqueous phase consisting of a very diluted solution of β-galactosidase and an appropriate fluorogenic substrate. At that time (1961), approximately 1 million fluorescent product molecules were needed for the detection of the catalytic reaction in the droplets. Although Rotman tried to measure the same droplets repeatedly every few hours, any dynamic disorder in the activity of individual enzymes was well hidden by time-averaging. The water-in-oil emulsion method for single-molecule enzymology was later rediscovered (54) and expanded with more modern technology, such as a CCD camera. These improvements allowed for better time resolution and enabled the simultaneous analysis of many droplets. Despite these improvements, the time resolution of this approach does not allow the detection of single enzymatic turnovers. Although each measurement point represents a time average over many turnovers, fluctuations in the rate of product formation were still detectable on a minute time scale, proving the validity of this approach.

4.3.3. Femtoliter array. The main disadvantage of the emulsion approach is that the droplets are not monodisperse in size. This problem can be overcome with arrays of microsized wells. These wells, whose volume is in the femtoliter range, can be prepared from various materials. They are filled by pipetting a diluted enzyme solution containing substrate on top of the array and then sealing the array with an appropriate lid. If the concentration is chosen correctly, one can deduce from Poissonian statistics that approximately 90% of the chambers end up empty and that most of the rest are filled with exactly one enzyme molecule.

The first such experiment was performed with wells etched into quartz glass to analyze the catalytic activity of lactate dehydrogenase (55). Later, soft lithography was used to prepare wells from polydimethylsiloxane for the analysis of β-galactosidase. Although these experiments represent primarily a first proof of principle, wells prepared in optical-fiber bundles have been used for a more detailed analysis of the enzymes β-galactosidase (15, 56) and HRP (57). The approach

based on optical-fiber bundles has the advantage that accumulated product molecules are excited by light traveling through the optical fiber. In the same way, the emitted fluorescence is recorded by a CCD camera after returning along the same optical path. Investigators have used experiments based on optical-fiber bundles to visualize the buildup of product molecules inside the wells by repeatedly taking images for a period of time. The fluorescence intensity for each well was plotted in time to obtain the average turnover frequency for each entrapped enzyme molecule.

In the β-galactosidase experiment (15), the average single-molecule K_M of 76 ± 23 μM was close to the value of 117 ± 23 μM found at the ensemble level. The average k_{cat} value of 916 ± 58 s^{-1} also compared well with the value of 888 ± 87 s^{-1} obtained from ensemble measurements. The distribution of velocities, however, was quite broad (coefficient of variation: 30%), indicating that not all enzymes in the population had the same activity. Furthermore, despite a low time resolution (seconds), fluctuations in the turnover rate were observed, indicating the presence of different enzyme conformations with interconversion rates on the second time scale (15). In the HRP experiment (57), the apparent substrate turnover rates for the single-enzyme experiments were ten times lower than in ensemble measurements. These low rates were attributed to a more complex reaction of the substrate Amplex® Red, which requires a two-step reaction to form the fluorescent dye resorufin. Whereas the first step of the reaction is enzyme catalyzed, the second step probably takes place outside the enzyme and is therefore susceptible to side reactions. The authors (57) point out that single-molecule data must be interpreted with care if the enzymatic reaction does not follow a one-step reaction with 1:1 stoichiometry for each reaction step to yield a fluorescent product molecule.

For all these measurements in impermeable containers or chambers, the size of the chamber must be carefully adjusted to ensure that substrate molecules are not depleted too quickly. Furthermore, depending on the choice of enzyme/substrate system, it is necessary to subtract a background caused by either photooxidation/autohydrolysis of the substrate to form the fluorescent product (positive background) or photobleaching of the fluorescent product (negative background). Photobleaching also defines the illumination intensity and the number of measurement points that can be taken. If the fluorescent dye bleaches faster than new product molecules are generated, no useful information can be obtained about the enzymatic reaction. In the HRP experiment, for example, the excitation intensity was chosen to be very low so that only very noisy single-enzyme time traces could be obtained. Despite these technical difficulties, the ability to perform highly parallel measurements of many individual enzymes at the same time makes the approach very powerful, and novel information about the observed enzymatic reactions has already been obtained.

4.4. Flow Assay in a Capillary

A third method that does not require immobilization of the enzyme is based on capillary electrophoresis. When a capillary is filled with a very dilute enzyme solution, the individual enzymes can be separated by centimeters. If this solution contains a fluorogenic substrate, fluorescent product molecules accumulate in proximity to the enzyme. After a certain incubation time, the enzyme and the generated product molecules are pulled through the capillary by electrophoresis. Fluorescent product molecules are detected as they are swept past a photodetector, thereby making it possible to determine how active each individual enzyme has been. With this approach, differences in the rate of product formation during the incubation time were detected for the enzymes lactate dehydrogenase (58), alkaline phosphatase (59), and β-galactosidase (60).

Initially, the incubation was performed while stopping the flow in the capillary. In the meantime, the approach was further developed for use under continuous-flow conditions (61). Exploiting the

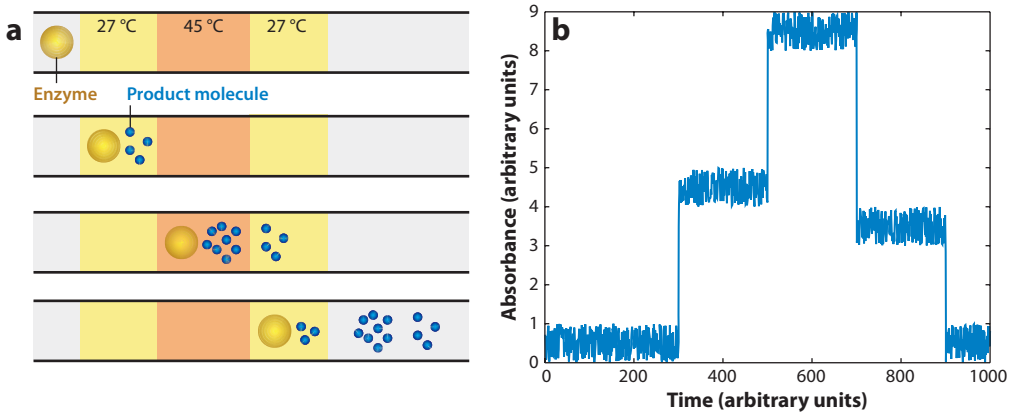

Figure 6

(*a*) Schematic drawing of an enzyme (*yellow*) moving through a capillary. At different temperatures, it produces product molecules (*blue*) at different rates. The product molecules move faster than the enzyme. (*b*) Simulated electropherogram arising from this bilevel temperature arrangement.

fact that the enzyme itself moves slower than the product molecules, investigators used the flow assay to vary the temperature along the capillary (**Figure 6**). With the product molecules running ahead of the enzyme, they are constantly separated from the enzyme and arrive at the detector in the order in which they were generated. Using this assay, researchers recorded a profile of the activity of several enzymes as they moved along the capillary; the time resolution was on the order of seconds. As a result of the variations in the temperature along the capillary, the shape of the activity profile showed that enzymes work harder at elevated temperatures. However, they are also more likely to become denaturated. A 20-s heat shock of 50°C denatured 45 of 53 β-galactosidase molecules. The surviving enzymes showed a 56 ± 10% residual activity, possibly caused by partial denaturation of the tetrameric enzyme. An important feature of this method is that it can be easily run unattended for large periods of time, allowing for the collection of numerous single-molecule profiles, which is vital for attaining proper statistics.

In summary, the flow assay is another elegant way to perform single-enzyme experiments with increased throughput, although again at the cost of a dramatically decreased time resolution. An interesting option may arise from a combination of emulsion technology with a flow assay based on microfluidics. The preparation and manipulation of emulsion droplets in microfluidic channels is a fast-developing new field (62, 63). Generated droplets are monodisperse and, if required, can even be kept stationary in the microfluidic system for a parallel kinetic observation (64). The detection of a single fluorescent molecule in an optically trapped emulsion droplet has recently been demonstrated (65). Through the use of high laser intensities, a product molecule can be bleached quickly, and the use of emulsion droplets may allow the detection of individual turnovers. In this context, new and exciting developments in single-molecule studies in droplet-based microfluidic systems can be expected.

5. CONCLUSIONS AND PERSPECTIVES

Having begun with the emulsion experiment of Rotman in the 1960s, the field of single-molecule enzymology has now advanced into the time-resolved age, and many different technological approaches have been developed to study the kinetics of a single enzyme. Independent of the

technological approach, differences in the activity between individual enzymes (static disorder) as well as fluctuations in the activity of each individual enzyme (dynamic disorder) have been observed over a broad range of time scales (up to seconds). In all cases studied, this disorder occurred on a functionally relevant time scale and did not contradict the Michaelis-Menten equation. Depending on the biological question to be answered, each of these technological approaches has its own advantages and disadvantages, and we currently do not know which approach will become a broadly applied method for examining individual enzymes. One must choose between a single-turnover time resolution combined with a low throughput or a highly parallel measurement with a drastically reduced time resolution.

Experiments with single-turnover resolution can reveal information about dynamic disorder in the activity of individual enzymes; for example, dynamic disorder may be observed as a nonexponential decay of the waiting times between individual turnovers. Dynamic disorder is further related to the observed memory effect, which indicates that different conformational states of an enzyme determine its rate of catalysis and that the waiting times between turnovers are correlated. This correlation is most easily explained with the fluctuating enzyme model, which has been introduced to visualize that the enzyme changes its conformation. The applied methods of data analysis, however, are still somewhat unsatisfactory. The autocorrelation function cannot provide information about the sequence of events, and the determination of the series of waiting times suffers from the problem of unambiguously assigning the on and off states in the time trace. In traces with a good signal-to-noise ratio, on and off states may be easily identified via the commonly used binning/thresholding approach. For lower-quality traces with a lot of Poissonian photon-counting noise, however, a trade-off is required. The bin size needs to be defined: The larger the bins are, the better the two states can be separated. At the same time, any fast events that occur within fractions of the bin time are averaged out. Also, the fact that the threshold is set arbitrarily is somewhat unsatisfactory. Lower-quality traces may benefit from a more objective method for obtaining binary trajectories such as change-point analysis (66, 67), in which a generalized likelihood ratio test is used to find the intensity change points. On the basis of the obtained waiting times for the on and off states, a number of groups of theoreticians are exploring the cause of the observed disorder and are developing approaches that make use of sequences of waiting times (21, 22, 68–71). These sequences may define certain (reoccurring) processes that take place while the enzyme is sampling functionally relevant conformational states. These theoretical approaches may allow for the reconstruction of an underlying kinetic scheme (69–71) or even of the energy landscape (21, 22). The reconstruction of kinetic schemes and energy landscapes becomes highly important when changes in activity are monitored as a function of regulation processes and mutations (see Section 2). So far, a small set of mostly commercially available enzyme-substrate systems has been used to show the usefulness of these different techniques. A clear correlation between consecutive turnovers was shown for many of these enzyme-substrate systems, indicating that the activity of an enzyme is not merely a stochastic process but rather is determined by conformational fluctuations that may directly affect its biological function. We are optimistic that the developed techniques will soon be used to explain how these fluctuations are influenced by mutations, ligand binding, and environmental effects and to ultimately gain a better understanding of the energy landscape and the structure-function-dynamics relationships that determine enzymatic reactions.

Leaving technological difficulties behind, the transition from in vitro to in vivo experiments would represent a significant development. Measurements will be complicated by the very high concentration of biomolecules in a cell and the scattering properties of tissues. To detect individual molecules in a cell, detection methods with high spatial resolution and extremely low background are required. Recent developments address both of these problems and may allow observation of single-enzyme activity in a cell. To address the problem of resolution, investigators have developed

several high-resolution imaging techniques that rely on the detection of individual fluorescent molecules (72–77). The first examples of imaging in living cells have recently been published (78, 79). On the basis of these technological developments, it may be possible to localize and monitor individual enzymes in a living cell, making use of the possibility to detect individual substrate turnovers. The problem involving a high fluorescence background in biological tissues could be solved with two-photon microscopy (**Figure 2*d***). This technique exploits the quantum-mechanically finite possibility that a fluorophore can absorb two (or more) lower-energy photons nearly simultaneously (80). Usually, infrared light—which is less prone to scattering than visible light—is used to excite fluorophores in the visible region of the spectrum. Moreover, the chance of multiphoton absorption is high only in the focus of the beam. The light is not able to excite molecules in other parts of the sample, thereby reducing these molecules' contribution to the background noise and making a pinhole superfluous. These advantages are further supported by the fact that lower-energy light is generally less likely to photobleach or otherwise damage the sample. Before the dream of detecting the kinetics of individual enzymes in a cell can become reality, better fluorescent reporter systems need to be developed. In addition to fulfilling the above-mentioned criteria, they need to be cell permeable and highly specific for the enzyme of interest to ensure that no side reactions can occur. These are crucial requirements that, of course, are not an issue with in vitro assays with purified enzymes.

DISCLOSURE STATEMENT

The authors are not aware of any affiliations, memberships, funding, or financial holdings that might be perceived as affecting the objectivity of this review.

ACKNOWLEDGMENTS

This work was supported by the Dutch National Research School Combination Catalysis Controlled by Chemical Design as well as a VIDI grant (K.B.) and a VICI grant (A.E.R) from the Netherlands Organisation for Scientific Research.

LITERATURE CITED

1. Michaelis L, Menten ML. 1913. Die Kinetik der Invertinwirkung. *Biochem. Z.* 49:333–69
2. Rotman B. 1961. Measurement of activity of single molecules of β-D-galactosidase. *Proc. Natl. Acad. Sci. USA* 47:1981–91
3. Frauenfelder H. 1995. Proteins—paradigms of complex systems. *Experientia* 51:200–3
4. Henzler-Wildman K, Kern D. 2007. Dynamic personalities of proteins. *Nature* 450:964–72
5. Dyson HJ, Wright PE. 2005. Intrinsically unstructured proteins and their functions. *Nat. Rev. Mol. Cell Biol.* 6:197–208
6. Sugase K, Dyson HJ, Wright PE. 2007. Mechanism of coupled folding and binding of an intrinsically disordered protein. *Nature* 447:1021–25
7. Vendruscolo M, Dobson CM. 2006. Dynamic visions of enzymatic reactions. *Science* 313:1586–87
8. Lu HP, Xun L, Xie XS. 1998. Single-molecule enzymatic dynamics. *Science* 282:1877–82
9. Edman L, Foldes-Papp Z, Wennmalm S, Rigler R. 1999. The fluctuating enzyme: a single molecule approach. *Chem. Phys.* 247:11–22
10. van Oijen AM, Blainey PC, Crampton DJ, Richardson CC, Ellenberger T, Xie XS. 2003. Single-molecule kinetics of λ exonuclease reveal base dependence and dynamic disorder. *Science* 301:1235–38
11. Velonia K, Flomenbom O, Loos D, Masuo S, Cotlet M, et al. 2005. Single-enzyme kinetics of CALB-catalyzed hydrolysis. *Angew. Chem. Int. Ed.* 44:560–64

12. Flomenbom O, Velonia K, Loos D, Masuo S, Cotlet M, et al. 2005. Stretched exponential decay and correlations in the catalytic activity of fluctuating single lipase molecules. *Proc. Natl. Acad. Sci. USA* 102:2368–72
13. English BP, Min W, van Oijen AM, Lee KT, Luo G, et al. 2006. Ever-fluctuating single enzyme molecules: Michaelis-Menten equation revisited. *Nat. Chem. Biol.* 2:87–94
14. Gumpp H, Puchner EM, Zimmermann JL, Gerland U, Gaub HE, Blank K. 2009. Triggering enzymatic activity with force. *Nano Lett.* 9:3290–95
15. Rissin DM, Gorris HH, Walt DR. 2008. Distinct and long-lived activity states of single enzyme molecules. *J. Am. Chem. Soc.* 130:5349–53
16. Eisenmesser EZ, Bosco DA, Akke M, Kern D. 2002. Enzyme dynamics during catalysis. *Science* 295:1520–23
17. Watt ED, Shimada H, Kovrigin EL, Loria JP. 2007. The mechanism of rate-limiting motions in enzyme function. *Proc. Natl. Acad. Sci. USA* 104:11981–86
18. Edman L, Rigler R. 2000. Memory landscapes of single-enzyme molecules. *Proc. Natl. Acad. Sci. USA* 97:8266–71
19. Hatzakis NS, Engelkamp H, Velonia K, Hofkens J, Christianen PC, et al. 2006. Synthesis and single enzyme activity of a clicked lipase-BSA hetero-dimer. *Chem. Commun.* 2006:2012–14
20. Engelkamp H, Hatzakis NS, Hofkens J, De Schryver FC, Nolte RJ, Rowan AE. 2006. Do enzymes sleep and work? *Chem. Commun.* 2006:935–40
21. Baba A, Komatsuzaki T. 2007. Construction of effective free energy landscape from single-molecule time series. *Proc. Natl. Acad. Sci. USA* 104:19297–302
22. Li CB, Yang H, Komatsuzaki T. 2008. Multiscale complex network of protein conformational fluctuations in single-molecule time series. *Proc. Natl. Acad. Sci. USA* 105:536–41
23. Gunasekaran K, Ma B, Nussinov R. 2004. Is allostery an intrinsic property of all dynamic proteins? *Proteins* 57:433–43
24. Boehr DD, Dyson HJ, Wright PE. 2006. An NMR perspective on enzyme dynamics. *Chem. Rev.* 106:3055–79
25. Boehr DD, Wright PE. 2008. How do proteins interact? *Science* 320:1429–30
26. Volkman BF, Lipson D, Wemmer DE, Kern D. 2001. Two-state allosteric behavior in a single-domain signaling protein. *Science* 291:2429–33
27. Formaneck MS, Ma L, Cui Q. 2006. Reconciling the "old" and "new" views of protein allostery: a molecular simulation study of chemotaxis Y protein (CheY). *Proteins* 63:846–67
28. Fersht AR. 1972. Conformational equilibria in α- and δ-chymotrypsin. The energetics and importance of the salt bridge. *J. Mol. Biol.* 64:497–509
29. Zhou HX, Rivas G, Minton AP. 2008. Macromolecular crowding and confinement: biochemical, biophysical, and potential physiological consequences. *Annu. Rev. Biophys.* 37:375–97
30. James LC, Tawfik DS. 2003. Conformational diversity and protein evolution—a 60-year-old hypothesis revisited. *Trends Biochem. Sci.* 28:361–68
31. Ishijima A, Kojima H, Funatsu T, Tokunaga M, Higuchi H, et al. 1998. Simultaneous observation of individual ATPase and mechanical events by a single myosin molecule during interaction with actin. *Cell* 92:161–71
32. Itoh H, Takahashi A, Adachi K, Noji H, Yasuda R, et al. 2004. Mechanically driven ATP synthesis by F_1-ATPase. *Nature* 427:465–68
33. Puchner EM, Alexandrovich A, Kho AL, Hensen U, Schäfer LV, et al. 2008. Mechanoenzymatics of titin kinase. *Proc. Natl. Acad. Sci. USA* 105:13385–90
34. Smiley RD, Hammes GG. 2006. Single molecule studies of enzyme mechanisms. *Chem. Rev.* 106:3080–94
35. Blank K, De Cremer G, Hofkens J. 2009. Fluorescence-based analysis of enzymes at the single-molecule level. *Biotechnol. J.* 4:465–79
36. Ballard JB, Carmichael ES, Shi D, Lyding JW, Gruebele M. 2006. Laser absorption scanning tunneling microscopy of carbon nanotubes. *Nano Lett.* 6:45–49
37. Funatsu T, Harada Y, Tokunaga M, Saito K, Yanagida T. 1995. Imaging of single fluorescent molecules and individual ATP turnovers by single myosin molecules in aqueous solution. *Nature* 374:555–59

38. Nishizaka T, Oiwa K, Noji H, Kimura S, Muneyuki E, et al. 2004. Chemomechanical coupling in F_1-ATPase revealed by simultaneous observation of nucleotide kinetics and rotation. *Nat. Struct. Mol. Biol.* 11:142–48
39. Adachi K, Oiwa K, Nishizaka T, Furuike S, Noji H, et al. 2007. Coupling of rotation and catalysis in F_1-ATPase revealed by single-molecule imaging and manipulation. *Cell* 130:309–21
40. Minsky M. 1988. Memoir on inventing the confocal scanning microscope. *Scanning* 10:128–38
41. Magde D, Elson EL, Webb WW. 1972. Thermodynamic fluctuations in a reacting system—measurement by fluorescence correlation spectroscopy. *Phys. Rev. Lett.* 29:705–8
42. Magde D, Elson EL, Webb WW. 1974. Fluorescence correlation spectroscopy. II. An experimental realization. *Biopolymers* 13:29–61
43. Ehrenberg M, Rigler R. 1974. Rotational brownian motion and fluorescence intensity fluctuations. *Chem. Phys.* 4:390–401
44. Krichevsky O, Bonnet G. 2002. Fluorescence correlation spectroscopy: the technique and its applications. *Rep. Prog. Phys.* 65:251–97
45. Schatzel K, Drewel M, Stimac S. 1988. Photon correlation measurements at large lag times: improving statistical accuracy. *J. Mod. Opt.* 35:711–18
46. Wahl M, Gregor I, Patting M, Enderlein J. 2003. Fast calculation of fluorescence correlation data with asynchronous time-correlated single-photon counting. *Opt. Express* 11:3583–91
47. Laurence TA, Fore S, Huser T. 2006. Fast, flexible algorithm for calculating photon correlations. *Opt. Lett.* 31:829–31
48. Kuznetsova S, Zauner G, Aartsma TJ, Engelkamp H, Hatzakis N, et al. 2008. The enzyme mechanism of nitrite reductase studied at single-molecule level. *Proc. Natl. Acad. Sci. USA* 105:3250–55
49. Rocha S, Hutchison JA, Peneva K, Herrmann A, Müllen K, et al. 2009. Linking phospholipase mobility to activity by single-molecule wide-field microscopy. *ChemPhysChem* 10:151–61
50. Hamdan SM, Loparo JJ, Takahashi M, Richardson CC, van Oijen AM. 2009. Dynamics of DNA replication loops reveal temporal control of lagging-strand synthesis. *Nature* 457:336–39
51. De Cremer G, Roeffaers MB, Baruah M, Sliwa M, Sels BF, et al. 2007. Dynamic disorder and stepwise deactivation in a chymotrypsin catalyzed hydrolysis reaction. *J. Am. Chem. Soc.* 129:15458–59
52. Reetz MT. 1997. Entrapment of biocatalysts in hydrophobic sol-gel materials for use in organic chemistry. *Adv. Mater.* 9:943–54
53. Comellas-Aragones M, Engelkamp H, Claessen VI, Sommerdijk NA, Rowan AE, et al. 2007. A virus-based single-enzyme nanoreactor. *Nat. Nanotechnol.* 2:635–39
54. Lee AI, Brody JP. 2005. Single-molecule enzymology of chymotrypsin using water-in-oil emulsion. *Biophys. J.* 88:4303–11
55. Tan WH, Yeung ES. 1997. Monitoring the reactions of single enzyme molecules and single metal ions. *Anal. Chem.* 69:4242–48
56. Gorris HH, Rissin DM, Walt DR. 2007. Stochastic inhibitor release and binding from single-enzyme molecules. *Proc. Natl. Acad. Sci. USA* 104:17680–85
57. Gorris HH, Walt DR. 2009. Mechanistic aspects of horseradish peroxidase elucidated through single-molecule studies. *J. Am. Chem. Soc.* 131:6277–82
58. Xue Q, Yeung ES. 1995. Differences in the chemical reactivity of individual molecules of an enzyme. *Nature* 373:681–83
59. Craig DB, Arriaga EA, Wong JCY, Lu H, Dovichi NJ. 1996. Studies on single alkaline phosphatase molecules: reaction rate and activation energy of a reaction catalyzed by a single molecule and the effect of thermal denaturation—the death of an enzyme. *J. Am. Chem. Soc.* 118:5245–53
60. Shoemaker GK, Juers DH, Coombs JM, Matthews BW, Craig DB. 2003. Crystallization of β-galactosidase does not reduce the range of activity of individual molecules. *Biochemistry* 42:1707–10
61. Craig DB, Nichols ER. 2008. Continuous flow assay for the simultaneous measurement of the electrophoretic mobility, catalytic activity and its variation over time of individual molecules of *Escherichia coli* β-galactosidase. *Electrophoresis* 29:4298–303
62. Kelly BT, Baret JC, Taly V, Griffiths AD. 2007. Miniaturizing chemistry and biology in microdroplets. *Chem. Commun.* 2007:1773–88

63. Schaerli Y, Hollfelder F. 2009. The potential of microfluidic water-in-oil droplets in experimental biology. *Mol. BioSyst.* 5:1392–404
64. Huebner A, Bratton D, Whyte G, Yang M, Demello AJ, et al. 2009. Static microdroplet arrays: a microfluidic device for droplet trapping, incubation and release for enzymatic and cell-based assays. *Lab Chip* 9:692–98
65. Tang J, Jofre AM, Lowman GM, Kishore RB, Reiner JE, et al. 2008. Green fluorescent protein in inertially injected aqueous nanodroplets. *Langmuir* 24:4975–78
66. Watkins LP, Yang H. 2005. Detection of intensity change points in time-resolved single-molecule measurements. *J. Phys. Chem. B* 109:617–28
67. Jansen M. 2007. Multiscale change point analysis in Poisson count data. *Chemom. Intell. Lab. Syst.* 85:159–69
68. Lerch HP, Rigler R, Mikhailov AS. 2005. Functional conformational motions in the turnover cycle of cholesterol oxidase. *Proc. Natl. Acad. Sci. USA* 102:10807–12
69. Witkoskie JB, Cao J. 2004. Single molecule kinetics. I. Theoretical analysis of indicators. *J. Chem. Phys.* 121:6361–72
70. Flomenbom O, Klafter J, Szabo A. 2005. What can one learn from two-state single-molecule trajectories? *Biophys. J.* 88:3780–83
71. Talaga DS. 2007. Markov processes in single molecule fluorescence. *Curr. Opin. Colloid Interface Sci.* 12:285–96
72. Betzig E, Patterson GH, Sougrat R, Lindwasser OW, Olenych S, et al. 2006. Imaging intracellular fluorescent proteins at nanometer resolution. *Science* 313:1642–45
73. Hess ST, Girirajan TPK, Mason MD. 2006. Ultra-high resolution imaging by fluorescence photoactivation localization microscopy. *Biophys. J.* 91:4258–72
74. Rust MJ, Bates M, Zhuang XW. 2006. Sub-diffraction-limit imaging by stochastic optical reconstruction microscopy (STORM). *Nat. Methods* 3:793–95
75. Folling J, Belov V, Kunetsky R, Medda R, Schonle A, et al. 2007. Photochromic rhodamines provide nanoscopy with optical sectioning. *Angew. Chem. Int. Ed.* 46:6266–70
76. Flors C, Hotta JI, Uji-I H, Dedecker P, Ando R, et al. 2007. A stroboscopic approach for fast photoactivation-localization microscopy with Dronpa mutants. *J. Am. Chem. Soc.* 129:13970–77
77. Heilemann M, van de Linde S, Schiittpelz M, Kasper R, Seefeldt B, et al. 2008. Subdiffraction–resolution fluorescence imaging with conventional fluorescent probes. *Angew. Chem. Int. Ed.* 47:6172–76
78. Shroff H, Galbraith CG, Galbraith JA, Betzig E. 2008. Live-cell photoactivated localization microscopy of nanoscale adhesion dynamics. *Nat. Methods* 5:417–23
79. Biteen JS, Thompson MA, Tselentis NK, Bowman GR, Shapiro L, Moerner WE. 2008. Super-resolution imaging in live *Caulobacter crescentus* cells using photoswitchable EYFP. *Nat. Methods* 5:947–49
80. Denk W, Strickler JH, Webb WW. 1990. Two-photon laser scanning fluorescence microscopy. *Science* 248:73–76

Annual Review of
Analytical Chemistry

Volume 3, 2010

Contents

Indexes

Errata

An online log of corrections to *Annual Review of Analytical Chemistry* articles may be found at http://arjournals.annualreviews.org/errata/anchem.